



Universidad Autónoma  
de Madrid

**Biblos-e Archivo**  
Repositorio Institucional UAM

**Repositorio Institucional de la Universidad Autónoma de Madrid**  
<https://repositorio.uam.es>

Esta es la **versión de autor** del artículo publicado en:  
This is an **author produced version** of a paper published in:

Translational Research 218 (2020): 43-56

**DOI:** <https://doi.org/10.1016/j.trsl.2019.12.004>

**Copyright:** © 2019 Elsevier Inc.

El acceso a la versión del editor puede requerir la suscripción del recurso  
Access to the published version may require subscription

# **PATHOGENIC IMPLICATIONS OF DYSREGULATED miRNAs IN PROPIONIC ACIDEMIA RELATED CARDIOMYOPATHY**

Alejandro Fulgencio-Covián<sup>1,2,3,4</sup>, Esmeralda Alonso-Barroso<sup>1,2,3,4</sup>, Adam J Guenzel<sup>5</sup>, Ana Rivera-Barahona<sup>1,2,3,4</sup>, Magdalena Ugarte<sup>2</sup>, Belén Pérez<sup>1,2,3,4</sup>, Michael A Barry<sup>5</sup>, Celia Pérez-Cerdá<sup>2,3,4</sup>, Eva Richard<sup>1,2,3,4</sup>, Lourdes R Desviat<sup>1,2,3,4</sup>

<sup>1</sup>Centro de Biología Molecular Severo Ochoa CSIC-UAM, Departamento de Biología Molecular, Universidad Autónoma de Madrid, Madrid, Spain

<sup>2</sup>Centro de Diagnóstico de Enfermedades Moleculares (CEDEM), Madrid, Spain

<sup>3</sup>Centro de Investigación Biomédica en Red de Enfermedades Raras (CIBERER), ISCIII

<sup>4</sup>Instituto de Investigación Sanitaria Hospital La Paz (IdiPaz), ISCIII

<sup>5</sup>Mayo Clinic, Rochester, Minnesota, USA

\*Correspondence to:

Lourdes R. Desviat (ORCID: 0000-0002-2081-0815)

Centro de Biología Molecular Severo Ochoa, UAM-CSIC

Universidad Autónoma de Madrid, 28049 Madrid, Spain.

Phone: +34 91 1964566

E-mail: lruiz@cbm.csic.es

***Running title: miRNAs in propionic acidemia related cardiomyopathy***

***Abbreviations:***

ANP: atrial natriuretic peptide

β-MHC: beta-myosin heavy chain

BNP: brain natriuretic peptide

CardiomiRs: cardiac enriched miRNAs

Ct: cycle threshold

DCM: dilated cardiomyopathy

EF: ejection fraction

FS: fractional shortening

GSK3: glycogen synthase kinase 3

HCM: hypertrophic cardiomyopathy

IGF-1: insulin-like growth factor 1

i.p.: intra peritoneal

IVRT: isovolumetric relaxation time

LV: left ventricle

LVID: left ventricle internal diameter

miRNA: microRNA

mTOR: mammalian target of rapamycin

MV: mitral valve

PA: propionic acidemia

PCC: propionyl-CoA carboxylase

PI3K/AKT: phosphatidylinositol 3 kinase-protein kinase B

ROS: reactive oxygen species

TEM: transmission electron microscopy

wt: wild-type

## Abstract

Cardiac alterations (hypertrophic/dilated cardiomyopathy, HCM/DCM, and rhythm alterations) are one of the major causes of mortality and morbidity in propionic acidemia (PA), caused by the deficiency of the mitochondrial enzyme propionyl-CoA carboxylase (PCC), involved in the catabolism of branched-chain amino acids, cholesterol and odd-chain fatty acids. Impaired mitochondrial oxidative phosphorylation has been documented in heart biopsies of PA patients, as well as in the hypomorphic *Pcca*<sup>-/-</sup>(A138T) mouse model, in the latter correlating with increased oxidative damage and elevated expression of cardiac dysfunction biomarkers atrial and brain natriuretic peptides (ANP and BNP) and beta-myosin heavy chain ( $\beta$ -MHC). Here we characterize the cardiac phenotype in the PA mouse model by histological and echocardiography studies and identify a series of upregulated cardiac-enriched microRNAs (miRNAs) in the PA mouse heart, some of them also altered as circulating miRNAs in PA patients' plasma samples. In PA mice hearts we show alterations in signaling pathways regulated by the identified miRNAs, which could be contributing to cardiac remodelling and dysfunction; notably, an activation of the mammalian target of rapamycin (mTOR) pathway and a decrease in autophagy, which are reverted by rapamycin treatment. *In vitro* studies in HL-1 cardiomyocytes indicate that propionate, the major toxic metabolite accumulating in the disease, triggers the increase in expression levels of miRNAs, BNP and  $\beta$ -MHC, concomitant with an increase in reactive oxygen species (ROS). Our results highlight miRNAs and signaling alterations in the PCC-deficient heart which may contribute to the development of PA-associated cardiomyopathy and provide a basis to identify new targets for therapeutic intervention.

**Keywords:** miRNAs, propionic acidemia, mTOR, cardiomyopathy, miR-208a, miR-199

## Introduction

MicroRNAs (miRNAs) are small non-coding RNAs that regulate gene expression through translational repression or transcript degradation via binding to complementary sequences in the 3'-UTR of target mRNAs. To date, evidence has accumulated identifying miRNA networks that govern most biological processes and signaling pathways in response to different stimuli [1]. Therefore, miRNA dysregulation negatively affects cellular physiology and contributes to disease development. Alterations in miRNA function have been reported in many human disorders including cancer, cardiovascular, neurodegenerative and metabolic diseases [2]. In addition to their role as critical contributors to cellular pathophysiology, the discovery of the stable presence of miRNAs in body fluids in relation to disease has laid the foundations for their clinical use as minimal invasive biomarkers for diagnosis, prognosis or treatment monitoring [3].

In inherited metabolic diseases different reports have described an altered miRNA profile in animal models and in patients' samples [2]. Plasma miRNA levels as biomarkers for disease and treatment response have been described [4], as well as modulation of miRNA levels as therapeutic approach [5]. In propionic acidemia (PA, MIM#606054), one of the most frequent life-threatening organic acidemias, caused by a defect in the mitochondrial enzyme propionyl-CoA carboxylase (PCC, E.C.6.4.1.3), we recently identified a set of altered miRNAs in liver of the hypomorphic mouse model *Pcca*<sup>-/-</sup>(A138T) [6]. Three of them, miR-34a, miR-338 and miR-350 were found upregulated in brain and heart tissue and the first two were also detected in altered levels in PA patients' plasma, underlying their possible contribution to disease pathophysiology and their potential as disease biomarkers [6].

PA results from mutations in either the *PCCA* or *PCCB* genes, encoding both subunits of the PCC enzyme, and is characterized by the toxic accumulation of propionyl-CoA and derived metabolites. This produces a secondary mitochondrial dysfunction, an energetic defect and cellular oxidative damage [7]. PA usually presents neonatally as a toxic encephalopathy although there are milder late-onset forms. Advances in supportive treatment based on protein restriction and carnitine supplementation have allowed patients to live beyond the neonatal period. However, the overall outcome remains poor in most patients, who suffer from numerous complications related to disease progression, among them cardiac alterations

(arrhythmias, dilated or hypertrophic cardiomyopathy (DCM or HCM)), a major cause of PA morbidity and mortality [8, 9]. The hypomorphic PA mouse model mimics the biochemical and clinical signs of the disease. It exhibits elevated expression of *Nppa*, *Nppb* and *Myh7*, encoding atrial natriuretic peptide (ANP), brain natriuretic peptide (BNP) and  $\beta$ -myosin heavy chain ( $\beta$ -MHC), respectively, biomarkers of cardiac dysfunction [6, 10]. Recently, using this model we have demonstrated the potential role of impaired  $\text{Ca}^{2+}$  handling in arrhythmias and cardiac dysfunction in PA [11].

Given these observations, in this study we have characterized the cardiac phenotype by histological and echocardiography studies in hypomorphic PA mice and analysed levels of cardiac enriched miRNAs (cardiomiRs), their target genes and regulated signaling pathways. Evidence of the clinical relevance of these findings was provided by the analysis of these cardiomiRs in PA patients' plasma samples. The results provide new insights into miRNA-mediated altered cellular processes involved in the development of PA-associated cardiomyopathy.

## Material and Methods

**Mice handling.** All mice used, wild-type (wt) and hypomorphic *Pcca*<sup>-/-</sup>(A138T), were adults (5-8 month-old) in an FVB background [10]. Both males and females were included in all experiments except in the echocardiographic analysis, in which only males were studied. Mice were maintained on standard chow. All the experiments were carried out in a pathogen-free environment at the Animal Facility of Centro de Biología Molecular Severo Ochoa, in accordance with the Spanish Law of Animal Protection. The Institutional Animal Experimentation Ethical Committee (Universidad Autónoma de Madrid, reference CEI 963-A026) and the Regional Environment Department (Comunidad de Madrid, reference PROEX 22/14) approved all animal experiments. Genomic DNA isolated from tail biopsies was used for animal genotyping, as previously described [10].

**Mice echocardiography.** Transthoracic echocardiography was blinded performed by an expert operator in the CNIC Imaging facility (<https://www.cnic.es/en/investigacion/imaging>) using a high-frequency ultrasound system (Vevo 2100, Visualsonics Inc., Canada) with a 40-MHz linear probe. Two-dimensional (2D) and M-mode (MM) echocardiography were performed at a frame rate above

230 frames/sec, and pulse wave Doppler (PW) was acquired with a pulse repetition frequency of 40 kHz. Mice were lightly anesthetized with 1-2% isoflurane in oxygen, adjusting the isoflurane delivery trying to maintain the heart rate in  $450\pm 50$  bpm. Mice were placed in supine position using a heating platform and warmed ultrasound gel was used to maintain normothermia. A base apex electrocardiogram was continuously monitored. Images were transferred to a computer and were analyzed off-line using the Vevo 2100 Workstation software.

For left ventricular (LV) systolic function assessment, parasternal standard 2D and MM, long and short axis views (LAX and SAX view, respectively) were acquired. LV ejection fraction, LV fractional shortening, and LV chamber dimensions were calculated from these views [12]. Mitral valve (MV) inflow pattern was acquired using PW Doppler echography in the 4-chamber apical view to assess diastolic function. The sample volume was positioned parallel to the blood flow, across the mitral orifice. Early and late diastolic velocity peak wave (E and A, respectively), the E/A ratio and isovolumetric relaxation time (IVRT) were measured [13].

**Transmission Electron Microscopy (TEM).** Cardiac tissue was collected immediately after mice were euthanized by exsanguination and placed in Trump's fixative (1% glutaraldehyde/4% formalin in 0.1M phosphate buffer), post-fixed in 1% osmium tetroxide, dehydrated in ethanol and embedded in Spurr epoxy resin. The tissue was sectioned at 800 angstroms, placed onto copper grids and stained with lead citrate. Sections were viewed using a model 1400 transmission electron microscope (JEOL, Tokyo, Japan) at an accelerating voltage of 80KeV.

**Rapamycin treatment.** Rapamycin (LC laboratories, Boston, Massachusetts, USA) was dissolved in ethanol at 20 mg/mL and diluted in a solution buffer of 90% PBS, 5% PEG 400, 5% Tween 80. 5 month-old wt and PA mice were injected intraperitoneally (i.p.) every day for a week with 2 mg/kg of rapamycin. After seven days of treatment, mice were sacrificed by CO<sub>2</sub> inhalation and hearts were excised, snap-frozen in liquid nitrogen and stored at -70°C until use.

**Human samples.** Human plasma samples were used for miRNA analysis. PA patients' plasma were remnants of samples referred to the laboratory for follow-up with the appropriate informed consent. Nine were from *PCCB* deficient patients and one from a *PCCA* deficient patient (Table 1). All the samples were taken during periods of metabolic stability of the patients and time after being diagnosed with DCM or Long Qt,

except for P5, who was diagnosed with emerging DCM at the time of plasma sampling. Matched control plasma samples were obtained from Sera Lab Ltd. (<http://www.seralab.co.uk/>), collected from consented anonymous donors. The Ethical Committee (Universidad Autónoma de Madrid) approved this study. All human experimental methods were performed in accordance with the relevant guidelines and regulations.

***Cell culture and propionate treatment.*** HL-1 cardiomyocytes were cultured in Claycomb medium (Sigma, Saint Louis, Missouri, USA), supplemented with 10% fetal bovine serum, glutamine 20 mM and a cocktail of antibiotics. To ensure proper growth of the cells, 0.3 M ascorbic acid (Sigma, Saint Louis, Missouri, USA), 1 mM retinoic acid (Sigma, Saint Louis, Missouri, USA) and 5 mg/mL insulin (Sigma, Saint Louis, Missouri, USA) were added to the medium. Before cell seeding, plates were treated for 24 hours with 0.1% gelatin and 25 µg of fibronectin (Sigma, Saint Louis, Missouri, USA). Three days before propionate treatment, cells were seeded in P6 plates (~200,000 cells per well). Then, 5 mM of sodium propionate (Sigma, Saint Louis, Missouri, USA) was added to the medium and refreshed at 48 hours. Cells were collected for mRNA and miRNA analysis and reactive oxygen species (ROS, H<sub>2</sub>O<sub>2</sub>) quantification four or eight days after initiation of treatment. To determine ROS production by flow cytometry, cells were detached by trypsinization and cellular fluorescence intensity was measured after 30 minutes incubation at 37 °C with the H<sub>2</sub>DCFDA probe in the FACS Canto II (Becton Dickinson Biosciences). Data analysis was performed using FlowJo program.

***RNA and protein extraction.*** For RNA extraction, both tissue and cell (HL-1 cardiomyocytes) samples were treated for 20 minutes with lysis buffer (supplied by Qiagen) and proteinase K. Then, total RNA was extracted using miRNeasy mini kit (QIAGEN, Hilden, Germany) according to manufacturer's instructions. Concentration and integrity of total RNA was measured in the NanoDrop ND-1000 spectrophotometer (NanoDrop Technologies Inc, Rockland, DE, USA). RNA isolation from human plasma samples was performed using miRNeasy Serum/Plasma Advanced Kit (QIAGEN, Hilden, Germany), following the manufacturer's instructions. 200 µL of plasma were used and RNA was eluted in 20 µL.

Protein samples were obtained from HL-1 cells and from frozen mouse heart tissue. HL-1 cells were harvested by trypsinization and treated with lysis buffer (10 mM Tris-



HCl 7.5, 150 mM NaCl, 0.1% Triton and 10% glycerol), protease and phosphatase inhibitors. Samples were subjected to freeze-thawing cycles and proteins were collected in the supernatant fraction after centrifugation of the cell lysates. Mouse heart tissue was pulverized using screws cooled in liquid N<sub>2</sub> and proteins were isolated by disrupting the powdered tissue in lysis buffer (50 mM Tris-HCl pH 7.5, 150 mM NaCl, 0.1% Triton X-100, 1 mM EDTA and 10% glycerol) using TissueLyser (two rounds of 90 seconds at 20 Hz) followed by centrifugation at 10,000 g for 30 minutes at 4°C. Protein concentration in the supernatant was measured using the Bradford method (Bio-Rad Laboratories).

**miRNA analysis.** 5 ng of total RNA obtained from heart tissue or HL-1 cells and 4 µL of the RNA eluate from plasma samples were used for retro-transcription using the miRCURY LNA RT Kit (QIAGEN, Hilden, Germany). miRNAs were amplified using specific LNA primers and miRCURY LNA SYBR Green PCR kit (QIAGEN, Hilden, Germany), in a LightCycler 480 instrument (Roche Applied Biosciences, In, USA), according to the manufacturer's instructions. For tissue and cellular samples, miR-423-3p and snRNA U6 were used as endogenous controls; for plasma samples, miR-103a-3p was used for normalization. Relative miRNA expression was quantified using the comparative threshold method after the detection of the different Ct values for the reference miRNA and the target ones, using the  $2^{-\Delta\Delta C_t}$  method. All samples were run in triplicate.

**mRNA quantification.** For gene expression analysis, cDNA was obtained by retrotranscription of 500 ng of total RNA from mouse heart samples or HL-1 cells using NZY First-Strand cDNA synthesis kit (NZYTech, Lda, Lisbon, Portugal). *Nppa* (ANP), *Nppb* (BNP), *Myh7* (β-MHC), *Col1a1* (COL1A1), *Col1a2* (COL1A2), *Col3a1* (COL3A1) and *Med13* (THRAP1) genes were amplified with specific primers (available upon request) using Perfecta SYBR Green FastMix kit (Quanta Biosciences, Beverly, MA, USA) in a LightCycler480 II instrument (Roche Applied Biosciences, In, USA). *Gapdh* was used as endogenous control and quantification was done using the  $2^{-\Delta\Delta C_t}$  method.

**Phosphatidylinositol 3 kinase-protein kinase B (PI3K/AKT) signaling pathway expression profiling.** Total RNA (100 ng/µL) from wt and PA mouse heart tissue was reversed transcribed using NZY First-Strand cDNA synthesis kit (NZYTech, Lda, Lisbon, Portugal). cDNA samples were pooled in four control and four PA groups.

mRNA profiling was performed with Mouse PI3K-AKT Signaling Pathway RT<sup>2</sup> Profiler PCR Array (QIAGEN, Hilden, Germany), which contains mouse specific primers for 84 genes involved in the PI3K-AKT pathway. Real-time PCR amplification was performed with Perfecta SYBR Green FastMix (Quanta Biosciences, Beverly, MA, USA) in an ABI 7900HT instrument (Applied Biosystems, CA, USA). The ABI software was used to obtain raw threshold cycle (Ct) value for each mRNA. qRT-PCR reactions and analysis were carried out at Genomics Core Facility, Parque Científico de Madrid, Spain. Relative quantification or fold change for each mRNA was calculating with the  $2^{-\Delta\Delta C_t}$  method, using 5 housekeeping genes (*Gapdh*, *B2m*, *Actb*, *Ywhah* and *Gusb*) as internal controls.

**Western blotting.** For western blot analysis, equal amounts of protein (50-75 µg) were loaded into 10% or 12% SDS-polyacrylamide gels. Proteins were transferred into a nitrocellulose membrane using the iBlot® Dry Blotting System. For the analysis of total and phosphorylated proteins, membranes were blocked for 1 hour with 5% non-fat milk or 3% BSA respectively, in 0.1% TBS-tween and incubated overnight with the corresponding primary antibody: LC3B (1:500, Cell Signaling Technology, Danvers, MA, USA), caspase 3, caspase 9, LAMP1, Phospho-p70 S6 Kinase (Thr389), p70 S6 Kinase, S6 Ribosomal Protein, Phospho-4E-BP1 (Ser65), Phospho-S6 Ribosomal Protein (Ser240/244), 4E-BP1 (all of them used at 1:1,000, Cell Signaling Technology, Danvers, MA, USA) and p62/SQSTM1 (2C11) (1:5,000, Abnova-novus biologicals, USA). Secondary antibodies were goat anti-rabbit and goat anti mouse (1:5,000 or 1:10,000 respectively, Santa Cruz Biotechnology, Santa Cruz, CA, USA). Antibody against GAPDH was used as loading control (1:5,000, Abcam, Cambridge, UK). Enhanced chemiluminescence reagent (ECL, GE Healthcare) was used for protein detection. Band intensity for each protein was quantified with BioRad GS-900 Densitometer (BioRad) and ImageLab program.

**Bioinformatics tools.** miRNA function, their targets and their expression profile were analyzed using miRWalk 2.0 (<http://zmf.umm.uni-heidelberg.de/apps/zmf/mirwalk2/>), TargetScan database ([http://www.targetscan.org/vert\\_72/](http://www.targetscan.org/vert_72/)) and Human miRNA Tissue Atlas (<https://ccb-web.cs.uni-saarland.de/tissueatlas/>).

**Statistical analysis.** Data were presented as mean ± SD. To analyze significant differences, the distribution of two groups was compared using two-tailed unpaired T-test distribution; three or more groups were compared using ANOVA method followed

by the Tukey's honestly significant difference (HSD) or Games Howell post hoc test. P values below 0.05 were considered statistically significant: \* $p < 0.05$ ; \*\* $p < 0.01$ ; \*\*\* $p < 0.001$ .

## Results

### Echocardiographic and biochemical studies

In order to characterize the cardiac phenotype of the hypomorphic PA mouse model, we performed echocardiographic studies in wt and *Pcca*<sup>-/-</sup>(A138T) male mice (n=6 wt group and n=7 PA group) at 5 and 8 months of age. Longitudinal echocardiographic analyses revealed cardiac alterations characterized by signs suggestive of diastolic dysfunction (Table 2). The diastolic interventricular septal thickness (IVS; d) was increased in PA mice compared with that of control mice. Diastolic left ventricular posterior wall thickness (LVPW; d) was also significantly increased in hypomorphic 5 month-old mice compared with wt mice. No differences were found in the analysis of the left ventricular mass (LV mass). E/A ratio, a clinical marker of diastolic dysfunction, was slightly increased in PA mice at 5 (35% increase) and 8 (20% increase) months of age as compared to wt (Table 2) not reaching statistical significance. In addition, PA mice had an elevation in left ventricle internal diameter (LVID) at end-diastole at both ages, indicating LV chamber dilation and DCM. We observed a reduction in the ejection fraction (EF) and fractional shortening (FS) parameters in 8 month-old PA mice compared to wt although not reaching statistical significance (Table 2). Heart rates were similar between wt and PA mice.

Further to functional abnormalities, PA mice also displayed elevated gene expression of the fibrosis markers *Col1a1* and *Col3a1* at 5 months of age (Supplementary Fig 1). The expression of *Nppa*, *Nppb* and *Myh7*, coding for cardiac damage markers ANP, BNP and  $\beta$ -MHC, is elevated at this time point [6, 10], with no statistically significant changes detected at earlier (2 months) or later (10 months) ages (data not shown).

### Histology and electron microscopy studies

Mitochondrial dysfunction inherent to PA can lead to lipid accumulation in tissue; lipid droplets have been observed in muscle tissue from PA patients [14]. Cardiac tissues from the mice were analyzed by TEM. Hearts from wt mice contained regular sarcomere banding patterns with mitochondria evenly dispersed in relatively

straight bands with no lipid droplets (Fig 1, top row). In contrast, there were increased numbers of light grey and white circular bodies consistent with the presence of lipid droplets in the hearts from PA mice (Fig 1, bottom rows).

### **Expression levels of cardiomiRs in PA mice hearts**

We selected a series of 13 miRNAs expressed in cardiac tissue and reported in the literature to be associated with cardiomyopathies (Supplementary Table 1) for their analysis in heart samples from wt and PA mice (n=5 per group, 5 month-old males and females). The results showed a significant upregulation of 11 miRNAs, with miR-208a, miR-22, miR-199a and miR-199b exhibiting the highest fold-increase (13-fold to 15-fold) compared to samples from wt mice (Fig 2). The expression of miR-208a in PA mice hearts was further examined at different ages, in 2 month-old mice there is a moderate increase (3-fold compared to wt mice) while in 10 month-old mice its expression is reduced (0.2-fold) (data not shown).

### **Analysis of signaling pathways and selected miRNA targets**

Our next aim was the investigation of altered cellular processes regulated by the identified miRNAs that could underlie the development of cardiomyopathy in PA. Thus, we analyzed signaling pathways and selected target genes of the miRNAs, previously functionally validated by modulating miRNA levels in different cellular and/or animal models of heart disease (Supplementary Table 1).

As a first step, we performed gene expression profiling in PA and wt mice heart samples (n=8, grouped in two pools of 4 mice each, 5 month-old males and females), analyzing 84 genes involved in the PI3K/AKT pathway that has been shown to play a role in cardiac remodelling [15] and is regulated by several of the identified cardiomiRs. The analysis included members of the AKT and PI3K families and their regulators, genes involved in regulation of actin organization and cell migration, glycogen synthase kinase 3 (GSK3) inactivation and  $\beta$ -catenin accumulation, and genes in the insulin-like growth factor 1 (IGF-1), mammalian target of rapamycin (mTOR), autophagy and apoptotic pathways. 18 genes were downregulated and 15 upregulated, considering fold changes of  $>1.3$  or  $<0.7$  (Fig 3). Among the upregulated genes there are several that promote cell survival/proliferation and/or with pro-hypertrophic function such as *Jun*, *Igf1r*, *Eif4b*, *Raf1*, *Pak1*, *Mtor*, *Plk3ca*, *Tcl1* or *Fos*. Genes involved in inflammatory responses were also found up-regulated (*Tlr4*, *Tirap*, *Myd88*). On the other hand, genes regulating apoptosis (*Csnk2a1*, *Fasl*, *Foxo3*) exhibited decreased expression, as well as

others regulating NF $\kappa$ B activation (*Chuk*, *Irak1*, *Nfkb1a*). *Gja1*, encoding gap junction protein alpha expressed in the heart left ventricle and important for contraction, was also found downregulated, as well as *Pten* and *Tsc2*, known inhibitors of the mTOR pathway. The observed downregulation of *Pten*, validated target of miR-22, correlates with the observed increased expression of this miRNA, which is essential for cardiac growth and remodelling in response to stress [16]. Other targets of the identified dysregulated miRNAs in PA mice hearts are indicated in Fig 3.

In a next step, we sought to analyze in depth cardiac autophagy and mTOR activation in PA mouse heart tissue, based on the results of the PI3K/AKT array and on the described involvement of the mTOR pathway in the regulation of cardiomyocyte cell size mediated by miR-199a [17], one of the miRNAs which we found most highly upregulated. The results showed a significant decrease in the autophagic marker LAMP1 and an increase in p62, indicating autophagy impairment (Fig 4A) as well as activation of components of the mTOR signaling pathways in PA mice heart compared to controls (Fig 4B). Activation signature of the mTOR pathway and autophagy decrease were validated using the commercially available drug rapamycin. Acute treatment with this mTOR inhibitor (seven consecutive daily i.p. injections with 2 mg/kg of rapamycin in wt and PA mice, n=9-10 per group) effectively reverted some of these alterations, increasing autophagy process (increasing levels of LAMP1 and decreasing levels of p62) (Fig 4C) and decreasing levels of proteins involved in mTOR pathway (Fig 4D). Notably, rapamycin treatment in PA mice decreased the expression of *Nppb* and *Myh7* (Supplementary Fig 2).

In addition, we also investigated specific previously functionally validated targets of the dysregulated miRNAs, which could be contributing to PA cardiac dysfunction. miR-199a has been described to regulate metabolic switching from fatty acid oxidation to glycolysis during heart remodelling, through repression of the expression of cardiac peroxisome proliferator-activated receptor  $\delta$  (PPAR $\delta$ ) [18]. miR-208a is involved in the control of cardiac contractility in response to stress or hypothyroidism through the inhibition of MED13, a cofactor of the thyroid hormone nuclear receptor that represses  $\beta$ -MHC expression in the adult heart [19]. miR-133a represses the expression of caspase 3 and caspase 9 protecting cardiomyocytes from oxidative stress-mediated cell death [15]. Caspase 3 has also been validated as a direct target of miR-378. Accordingly, in PA mice heart, we could confirm a significant

decrease in the expression of these targets (*Ppard*, *Med13*, *Casp3* and *Casp9*) (Supplementary Fig 3).

### **Effect of propionate in HL-1 cardiomyocytes**

To investigate potential mechanisms triggering miRNA dysregulation in PA mice hearts and the contribution of accumulating toxic metabolites to the development of cardiac dysfunction, we analyzed the effect of propionate treatment in the cardiac murine cell line HL-1. Cells were treated during 4 days with 5 mM propionate (concentration detected in patients' plasma [20]) and the 4 miRNAs showing highest upregulation in PA mice hearts (miR-208a, miR-199b, miR-22 and miR-199a) were analyzed, as well as cardiac dysfunction markers and ROS levels. Propionate treatment resulted in an increase in ROS levels, as previously reported in different *in vitro* and *in vivo* models [7] and induced the expression of *Nppb* and *Myh7* (Fig 5A and 5B). miRNA levels did not vary significantly after 4 days but longer exposures to propionate (8 days) resulted in the upregulation of miR-22, miR-199a and miR-199b, while miR-208a levels decreased (Fig 5C).

### **miRNA analysis in PA patients' plasma samples**

Up to 70% of PA patients develop cardiomyopathy [8, 9]. In order to determine the translatability of the results obtained in the mouse model we investigated the presence and the expression levels of the identified cardiomiRs in PA patients' plasma samples compared to matched control samples (>12 years of age; n=10) (Table 1). In this preliminary study we analyzed 5 miRNAs showing highest upregulation in PA mice hearts (miR-208a, miR-22, miR-199a, miR-199b and miR-29a) as well as miR-133a, a circulating miRNA studied in relation to fibrosis and DCM [21]. miR-208a and miR-199b could not be detected, which in the case of miR-208a could be attributed to the specific amplification technique used [22]. miR-22, miR-29a, miR-133a and miR-199a were decreased in PA patients' samples (Fig 6A). Closer inspection of the miRNA profile in individual patient samples revealed a specific pattern shared by most of them (Fig 6B), even though not all patients exhibited the same cardiac phenotype (Table 1). Only patient 2 showed a clearly different miRNA profile with highly increased levels of miR-29a (Fig 6B).

### **Discussion**

Cardiomyopathy is a major health problem in PA patients, strongly influencing overall morbidity and mortality [8, 9]. Although PA usually presents neonatally and is today included in newborn screening programs in some countries, there are cases of milder, even asymptomatic, patients presenting later with cardiomyopathy. To date, it is largely accepted that the bioenergetic deficiency and oxidative stress due to a secondary mitochondrial dysfunction contributes to the progressive decline of myocardial function in PA. We have recently shown redox-mediated alterations in sarco/endoplasmic reticulum  $\text{Ca}^{2+}$ -ATPase (SERCA2a) function impairing  $\text{Ca}^{2+}$  handling as a new pathological mechanism involved in PA cardiomyopathy [11], although additional factors are probably involved. There is an unmet clinical need to advance further in the understanding of PA cardiac pathology, to develop novel, better suited treatments and to identify biomarkers for earlier diagnosis of this complication and for response to treatment. miRNAs are known to play an important role in cardiac development, dysfunction and failure. In this study we used the hypomorphic *Pcca*<sup>-/-</sup>(A138T) PA mouse model to analyze the expression of cardiac enriched miRNAs and their targets governing biological processes linked to cardiovascular disease.

Our results show structural defects and signs of diastolic dysfunction in PA mouse hearts and confirm the presence of specific markers of cardiac damage, including i) gene expression reprogramming, as shown by upregulation of early immediate genes (*c-Fos*, *Jun*) and reactivation of a set of fetal cardiac genes (*Nppb* and *Myh7*), ii) increase in the expression of collagen genes indicating the appearance of myocardial fibrosis, and iii) increase in protein synthesis and decrease in autophagy (mTOR activation). In addition, we observe a decrease in caspases 3 and 9 levels, indicative of cardiac remodeling that accompanies the progression of cardiac pathology. We could also confirm a significant decrease in the expression of *Ppard*, coding for PPAR $\delta$ , the critical regulator of energy metabolism in heart, which is shifted towards glycolysis in the failing heart. In line with this, we previously documented a significant reduction in the fatty acid oxidation enzyme HADHA in PA mouse hearts [23]. In brief, the data reflect the complex cellular phenotype with multiple signaling pathways altered in PA mouse hearts.

Notably, this is the first study describing the *in vivo* dysregulation of cardiac-enriched miRNAs in PA which could be involved in the development of cardiac alterations. We sought for potential causes and consequences of those changes and

identified propionate as an exogenous factor which may trigger the alterations in the expression of these miRNAs, although other mechanisms may act in concert. miRNA expression is regulated at both transcriptional and post-transcriptional levels, with documented direct and indirect effects of certain endogenous (chemokines, hormones) and exogenous (xenobiotics) compounds [24]. Propionate is a known histone deacetylase inhibitor [25] and cardiac remodelling and hypertrophy has been linked to histone acetylation [26]. In addition, propionyl-CoA was recently shown to stimulate transcription through an increase in histone 3 lysine propionylation (H3K4pr), thereby linking the metabolic state of the cell with chromatin architecture [27]. Livers of the hypomorphic PA mouse model display higher levels of H3K14pr which revert to wild-type levels after gene therapy [27]. Another plausible explanation is that miRNA dysregulation may be driven by a ROS signaling mechanism, as increased propionate levels induce ROS elevation resulting in oxidative damage, both *in vivo* and *in vitro* as shown in this work and in previous studies [28]. In turn, ROS are known to activate signaling kinases and transcription factors, mediate apoptosis and stimulate cardiac fibroblast proliferation leading to cardiac remodelling [29].

Eleven of the studied miRNAs were found upregulated in the PA mouse heart, with miR-208a, miR-199b, miR-22, miR-199a and showing >13-fold increased levels compared to wt samples. Except for miR-208a, the expression of these miRNAs was induced in cardiomyocytes upon propionate treatment. miR-208a plays a crucial role in heart health and disease, regulating cardiac contractility, hypertrophy pathway components and cardiac conduction system. It is encoded by an intron of the *Myh6* gene and upon cardiac stress induces the expression of the dominant embryonic myosin isoform  $\beta$ -MHC (which we find increased in PA mouse hearts), contributing to diminishing cardiac performance [19]. In DCM patients this miRNA has been described as a predictor of cardiac death and progression of heart failure, with higher endomyocardial levels associated with adverse clinical outcomes [30]. Recently, a negative feedback loop between ROS and miR-208a was recently shown in cultured rat cardiomyocytes, with ROS attenuating miR-208a expression [31], which could explain our results in propionate treated cardiomyocytes.

miR-199a is involved in mTOR activation and autophagy and in mitochondrial fatty-acid oxidation impairment [17, 18]. We have confirmed decreased *Ppard* expression, a direct target of miR-199a mediating cardiac fuel switch from fatty acid to



glucose, which is also observed in normal rat hearts perfused with high exogenous propionate [32], again providing a possible link between the accumulating metabolite in PA, a dysregulated miRNA and developing heart failure. Our data have also revealed an impairment in the autophagic flux in PA mouse hearts due to elevated mTOR signaling, which could contribute to cardiac pathology and that could be restored by rapamycin. Rapamycin ester temsirolimus, an FDA-approved drug with more favorable pharmaceutical properties and mild side effects [33], may be an attractive therapeutic option for PA patients exhibiting cardiomyopathy.

Furthermore, the miRNAs identified in our study can be considered *per se* as potential therapeutic targets. miRNA-based therapeutics is currently an increasing field of research, with the development of drugs aiming to inhibit (antagomiRs) or overexpress (miRNA mimics) specific miRNAs altered in disease [34]. Future studies will elucidate whether this approach is applicable in the PA mouse model, due to the observed complex changes in different cellular processes regulated by multiple miRNAs. In DCM, few miRNAs have been directly implicated as therapeutic targets, although the overexpression of miR-699a resulting in a long-term benefit for severe chronic myotonic dystrophy-associated DCM represents a landmark case [35].

The presence of dysregulated circulating cardiomiRs in PA patients' samples provides strong evidence of the clinical significance of our study. As in other diseases [36] we observe opposed changes in expression in tissues versus plasma samples (upregulated and downregulated, respectively), which can be due to different regulatory processes in mice and humans, as well as to the fact that miRNAs are mostly actively secreted as a specific biological process and circulating miRNAs do not reflect intracellular levels. Although the low number of samples analyzed (a common limitation in the field of rare genetic diseases) precludes drawing definitive conclusions, the distinct miRNA signatures also support their potential applicability as biomarkers of disease progression or of response to treatment. However, given the low concentration of circulating cardiomiRs in plasma samples, which is further decreased in PA patients, the use of alternative profiling methods such as next generation sequencing which may provide lower detection limits and accurate quantification [37], should be evaluated and differences rigorously validated. It is worth noting that some of the patients showing an altered circulating miRNA profile exhibited no cardiac manifestations at the time of the analysis and that the only patient under specific treatment for cardiac disease exhibits a

different miRNA profile (P2 in Fig 6B). Our results constitute a starting point for a wider international study including different PA patient cohorts with documented clinical histories relative to cardiac phenotypes. It will be interesting to confirm if early metabolic and signaling dysregulations and miRNA and gene expression alterations precede overt cardiomyopathy in PA, as has been documented for other monogenic diseases [38]. In addition and as cardiomyopathies may be reversed after liver transplantation in PA patients [39], the analysis of circulating cardiomiRs before and after this intervention will confirm the involvement of these miRNAs in PA-associated cardiomyopathy.

## **ACKNOWLEDGEMENTS**

The technical assistance of Elena Montalvo and the expert advice of the staff at CNIC Imaging Facility are gratefully acknowledged. The authors thank Federación Española de Enfermedades Metabólicas Hereditarias and the patients' families for their collaboration and for agreeing to participate in the study. This work was supported by Spanish Ministry of Economy and Competitiveness and European Regional Development Fund (grant number SAF2016-76004-R) and by Fundación Isabel Gemio and Fundación La Caixa (LCF/PR/PR16/11110018). AFG is funded by the FPI-UAM program, EAB and ARB by the Spanish Ministry of Science, Innovation and Universities (predoctoral fellowships FPU15/02923 and BES-2014-069420, respectively). Centro de Biología Molecular Severo Ochoa receives an institutional grant from Fundación Ramón Areces.

The authors are aware of the journal's authorship statement and declare no conflict of interest. All authors have read and approved the final version of the manuscript.

## REFERENCES

- [1] Gosline SJ, Gurtan AM, JnBaptiste CK, Bosson A, Milani P, Dalin S, et al. Elucidating MicroRNA Regulatory Networks Using Transcriptional, Post-transcriptional, and Histone Modification Measurements. *Cell reports*. 2016;14:310-9.
- [2] Rivera-Barahona A, Perez B, Richard E, Desviat LR. Role of miRNAs in human disease and inborn errors of metabolism. *J Inherit Metab Dis*. 2017;40:471-80.
- [3] De Guire V, Robitaille R, Tetreault N, Guerin R, Menard C, Bambace N, et al. Circulating miRNAs as sensitive and specific biomarkers for the diagnosis and monitoring of human diseases: promises and challenges. *Clin Biochem*. 2013;46:846-60.
- [4] Li Y, Peng T, Li L, Wang X, Duan R, Gao H, et al. MicroRNA-9 regulates neural apoptosis in methylmalonic acidemia via targeting BCL2L1. *Int J Dev Neurosci*. 2014;36:19-24.
- [5] Frankel LB, Di Malta C, Wen J, Eskelinen EL, Ballabio A, Lund AH. A non-conserved miRNA regulates lysosomal function and impacts on a human lysosomal storage disorder. *Nature communications*. 2014;5:5840.
- [6] Rivera-Barahona A, Fulgencio-Covian A, Perez-Cerda C, Ramos R, Barry MA, Ugarte M, et al. Dysregulated miRNAs and their pathogenic implications for the neurometabolic disease propionic acidemia. *Sci Rep*. 2017;7:5727.
- [7] Richard E, Perez B, Perez-Cerda C, Desviat LR. Understanding molecular mechanisms in propionic acidemia and investigated therapeutic strategies. *Expert Opinion on Orphan Drugs*. 2015;3:1427-38.
- [8] Pena L, Burton BK. Survey of health status and complications among propionic acidemia patients. *Am J Med Genet A*. 2012;158A:1641-6.
- [9] Haijes HA, Jans JJM, Tas SY, Verhoeven-Duif NM, van Hasselt PM. Pathophysiology of propionic and methylmalonic acidemias. Part 1: Complications. *J Inherit Metab Dis*. 2019;42:730-44.
- [10] Guenzel AJ, Hofherr SE, Hillestad M, Barry M, Weaver E, Venezia S, et al. Generation of a hypomorphic model of propionic acidemia amenable to gene therapy testing. *Mol Ther*. 2013;21:1316-23.
- [11] Tamayo M, Fulgencio-Covian A, Navarro-Garcia JA, Val-Blasco A, Ruiz-Hurtado G, Gil-Fernandez M, et al. Intracellular calcium mishandling leads to cardiac

- dysfunction and ventricular arrhythmias in a mouse model of propionic acidemia. *Biochim Biophys Acta Mol Basis Dis.* 2020;1866:165586.
- [12] Moran CM, Thomson AJ, Rog-Zielinska E, Gray GA. High-resolution echocardiography in the assessment of cardiac physiology and disease in preclinical models. *Exp Physiol.* 2013;98:629-44.
- [13] Schnelle M, Catibog N, Zhang M, Nabeebaccus AA, Anderson G, Richards DA, et al. Echocardiographic evaluation of diastolic function in mouse models of heart disease. *J Mol Cell Cardiol.* 2018;114:20-8.
- [14] Schwab MA, Sauer SW, Okun JG, Nijtmans LG, Rodenburg RJ, van den Heuvel LP, et al. Secondary mitochondrial dysfunction in propionic aciduria: a pathogenic role for endogenous mitochondrial toxins. *Biochem J.* 2006;398:107-12.
- [15] Wang J, Liew OW, Richards AM, Chen YT. Overview of MicroRNAs in Cardiac Hypertrophy, Fibrosis, and Apoptosis. *Int J Mol Sci.* 2016;17.
- [16] Xu XD, Song XW, Li Q, Wang GK, Jing Q, Qin YW. Attenuation of microRNA-22 derepressed PTEN to effectively protect rat cardiomyocytes from hypertrophy. *J Cell Physiol.* 2012;227:1391-8.
- [17] Li Z, Song Y, Liu L, Hou N, An X, Zhan D, et al. miR-199a impairs autophagy and induces cardiac hypertrophy through mTOR activation. *Cell Death Differ.* 2017;24:1205-13.
- [18] el Azzouzi H, Leptidis S, Dirkx E, Hoeks J, van Bree B, Brand K, et al. The hypoxia-inducible microRNA cluster miR-199a-214 targets myocardial PPARdelta and impairs mitochondrial fatty acid oxidation. *Cell Metab.* 2013;18:341-54.
- [19] Callis TE, Pandya K, Seok HY, Tang RH, Tatsuguchi M, Huang ZP, et al. MicroRNA-208a is a regulator of cardiac hypertrophy and conduction in mice. *J Clin Invest.* 2009;119:2772-86.
- [20] Feliz B, Witt DR, Harris BT. Propionic acidemia: a neuropathology case report and review of prior cases. *Arch Pathol Lab Med.* 2003;127:e325-8.
- [21] Rubis P, Toton-Zuranska J, Wisniowska-Smialek S, Holcman K, Kolton-Wroz M, Wolkow P, et al. Relations between circulating microRNAs (miR-21, miR-26, miR-29, miR-30 and miR-133a), extracellular matrix fibrosis and serum markers of fibrosis in dilated cardiomyopathy. *Int J Cardiol.* 2017;231:201-6.
- [22] Sygitowicz G, Tomaniak M, Blaszczyk O, Koltowski L, Filipiak KJ, Sitkiewicz D. Circulating microribonucleic acids miR-1, miR-21 and miR-208a in patients with

- symptomatic heart failure: Preliminary results. *Arch Cardiovasc Dis.* 2015;108:634-42.
- [23] Gallego-Villar L, Rivera-Barahona A, Cuevas-Martin C, Guenzel A, Perez B, Barry MA, et al. In vivo evidence of mitochondrial dysfunction and altered redox homeostasis in a genetic mouse model of propionic acidemia: Implications for the pathophysiology of this disorder. *Free Radic Biol Med.* 2016;96:1-12.
- [24] Gulyaeva LF, Kushlinskiy NE. Regulatory mechanisms of microRNA expression. *J Transl Med.* 2016;14:143.
- [25] Silva LG, Ferguson BS, Avila AS, Faciola AP. Sodium propionate and sodium butyrate effects on histone deacetylase (HDAC) activity, histone acetylation, and inflammatory gene expression in bovine mammary epithelial cells. *J Anim Sci.* 2018;96:5244-52.
- [26] Bagchi RA, Weeks KL. Histone deacetylases in cardiovascular and metabolic diseases. *J Mol Cell Cardiol.* 2019;130:151-9.
- [27] Kebede AF, Nieborak A, Shahidian LZ, Le Gras S, Richter F, Gomez DA, et al. Histone propionylation is a mark of active chromatin. *Nat Struct Mol Biol.* 2017;24:1048-56.
- [28] Richard E, Gallego-Villar L, Rivera-Barahona A, Oyarzabal A, Perez B, Rodriguez-Pombo P, et al. Altered Redox Homeostasis in Branched-Chain Amino Acid Disorders, Organic Acidurias, and Homocystinuria. *Oxid Med Cell Longev.* 2018;2018:1246069.
- [29] Tsutsui H, Kinugawa S, Matsushima S. Oxidative stress and heart failure. *Am J Physiol Heart Circ Physiol.* 2011;301:H2181-90.
- [30] Satoh M, Minami Y, Takahashi Y, Tabuchi T, Nakamura M. Expression of microRNA-208 is associated with adverse clinical outcomes in human dilated cardiomyopathy. *J Card Fail.* 2010;16:404-10.
- [31] Liu A, Sun Y, Yu B. MicroRNA-208a Correlates Apoptosis and Oxidative Stress Induced by H<sub>2</sub>O<sub>2</sub> through Protein Tyrosine Kinase/Phosphatase Balance in Cardiomyocytes. *Int Heart J.* 2018;59:829-36.
- [32] Wang Y, Christopher BA, Wilson KA, Muoio D, McGarrah RW, Brunengraber H, et al. Propionate-induced changes in cardiac metabolism, notably CoA trapping, are not altered by l-carnitine. *Am J Physiol Endocrinol Metab.* 2018;315:E622-E33.
- [33] Roskoski R, Jr. Properties of FDA-approved small molecule protein kinase inhibitors. *Pharmacol Res.* 2019;144:19-50.

- [34] Christopher AF, Kaur RP, Kaur G, Kaur A, Gupta V, Bansal P. MicroRNA therapeutics: Discovering novel targets and developing specific therapy. *Perspect Clin Res*. 2016;7:68-74.
- [35] Quattrocchi M, Crippa S, Montecchiani C, Camps J, Cornaglia AI, Boldrin L, et al. Long-term miR-669a therapy alleviates chronic dilated cardiomyopathy in dystrophic mice. *J Am Heart Assoc*. 2013;2:e000284.
- [36] Roberts TC, Blomberg KE, McClorey G, El Andaloussi S, Godfrey C, Betts C, et al. Expression analysis in multiple muscle groups and serum reveals complexity in the microRNA transcriptome of the mdx mouse with implications for therapy. *Mol Ther Nucleic Acids*. 2012;1:e39.
- [37] Mestdagh P, Hartmann N, Baeriswyl L, Andreasen D, Bernard N, Chen C, et al. Evaluation of quantitative miRNA expression platforms in the microRNA quality control (miRQC) study. *Nat Methods*. 2014;11:809-15.
- [38] Khairallah M, Khairallah R, Young ME, Dyck JR, Petrof BJ, Des Rosiers C. Metabolic and signaling alterations in dystrophin-deficient hearts precede overt cardiomyopathy. *J Mol Cell Cardiol*. 2007;43:119-29.
- [39] Romano S, Valayannopoulos V, Touati G, Jais JP, Rabier D, de Keyser Y, et al. Cardiomyopathies in propionic aciduria are reversible after liver transplantation. *J Pediatr*. 2010;156:128-34.

## LEGENDS TO FIGURES

**Figure 1. Transmission electron microscopy of cardiac tissue.** Heart tissue of wt and PA mice was analyzed by TEM. Panels on the left were viewed at 5,000X magnification, with bars representing 5  $\mu$ m. Panels on the right correspond to the image within the boxes shown at 20,000X magnification, with bars representing 1  $\mu$ m.

**Figure 2. Relative expression analysis of selected miRNAs specifically expressed in cardiac tissue (cardiomiRs).** miRNA expression analysis was performed by qRT-PCR in heart samples from wt and PA mice (5 month-old, n=5 per group). Statistical significance was determined by Student's t-test. \* $p<0.05$ ; \*\* $p<0.01$ , \*\*\* $p<0.001$ . RQ: relative quantity.

**Figure 3. Dysregulated genes in PA mice hearts identified in the expression array of PI3K/Akt signaling pathway.** Gene expression analysis was performed by qRT-PCR from cardiac pooled samples of wt and PA mice (5 month-old, n=8 per group). Upregulated miRNAs identified in PA mice hearts are shown above their respective targets.

**Figure 4. Analysis of protein levels of autophagy and the mTOR related signaling pathways.** Heart samples from 5 month-old wt and PA mice (n=5-10 per group) were analyzed by Western blot. Representative blots are shown on the left and on the right the corresponding quantification by laser densitometry of proteins involved in autophagy (LC3BI, LC3BII, LAMP1 and p62) (**A**, **C**) and protein synthesis (S6K, S6, 4EBP1, and the phosphorylated forms) (**B**, **D**). In each blot, GAPDH was used as a loading control. In C and D, protein values are shown relative to untreated controls. Statistical significance was determined by Student's t-test. \* $p<0.05$ ; \*\* $p<0.01$ , \*\*\* $p<0.001$ .

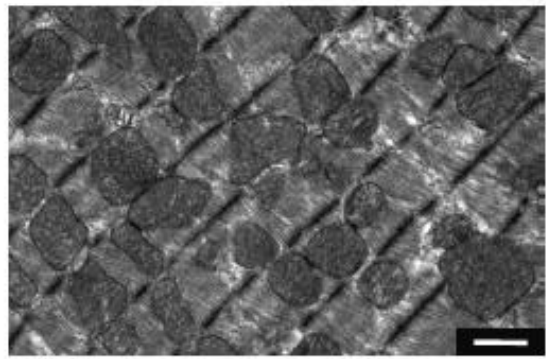
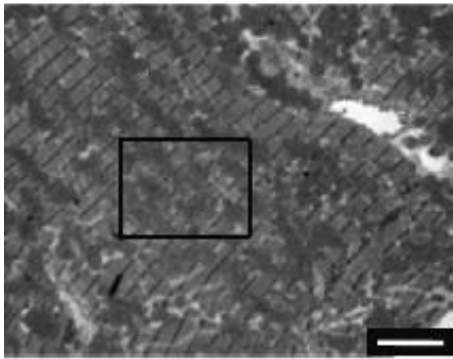
**Figure 5. Effect of propionate in the cardiac murine cell line HL-1.** Cells were treated with 5mM propionate for 4 days and (**A**) ROS production was quantified by flow cytometry using the H<sub>2</sub>DCFDA probe, (**B**) expression of cardiac damage markers *Nppb* and *Myh7* were analyzed by qRT-PCR. (**C**) cardiomiRs (miR-22, miR-199a/b and miR-208a) were analyzed by qRT-PCR after 4 and 8 days of propionate treatment.



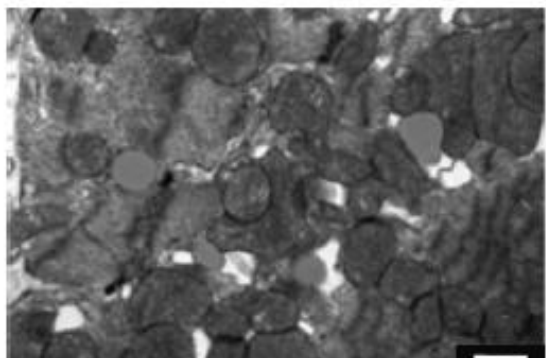
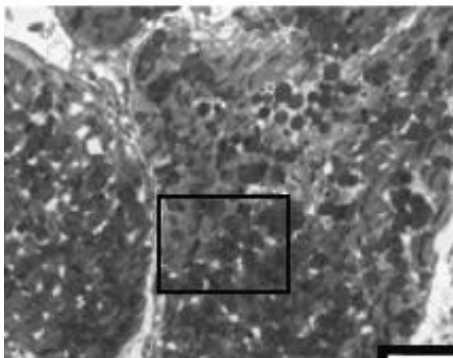
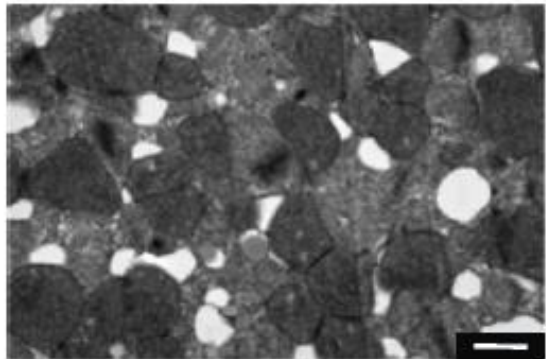
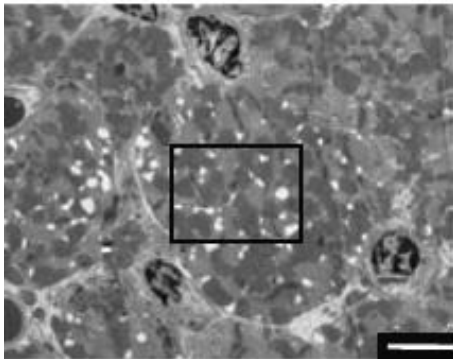
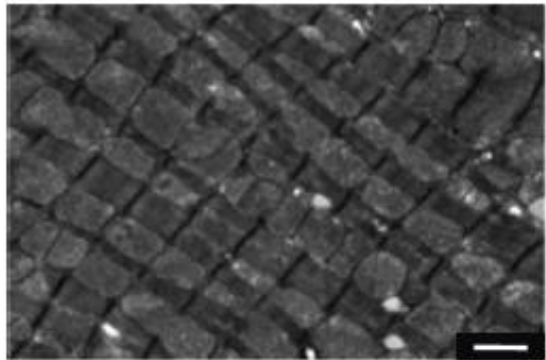
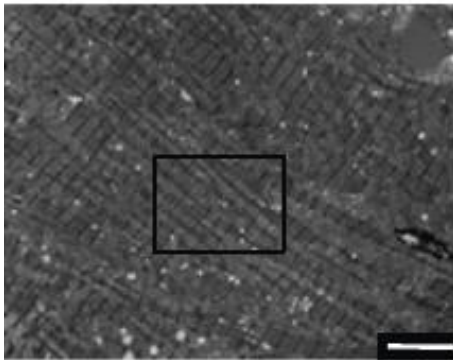
Statistical significance was determined by Student's t-test.  $**p<0.01$ ,  $***p<0.001$ . RQ: relative quantity.

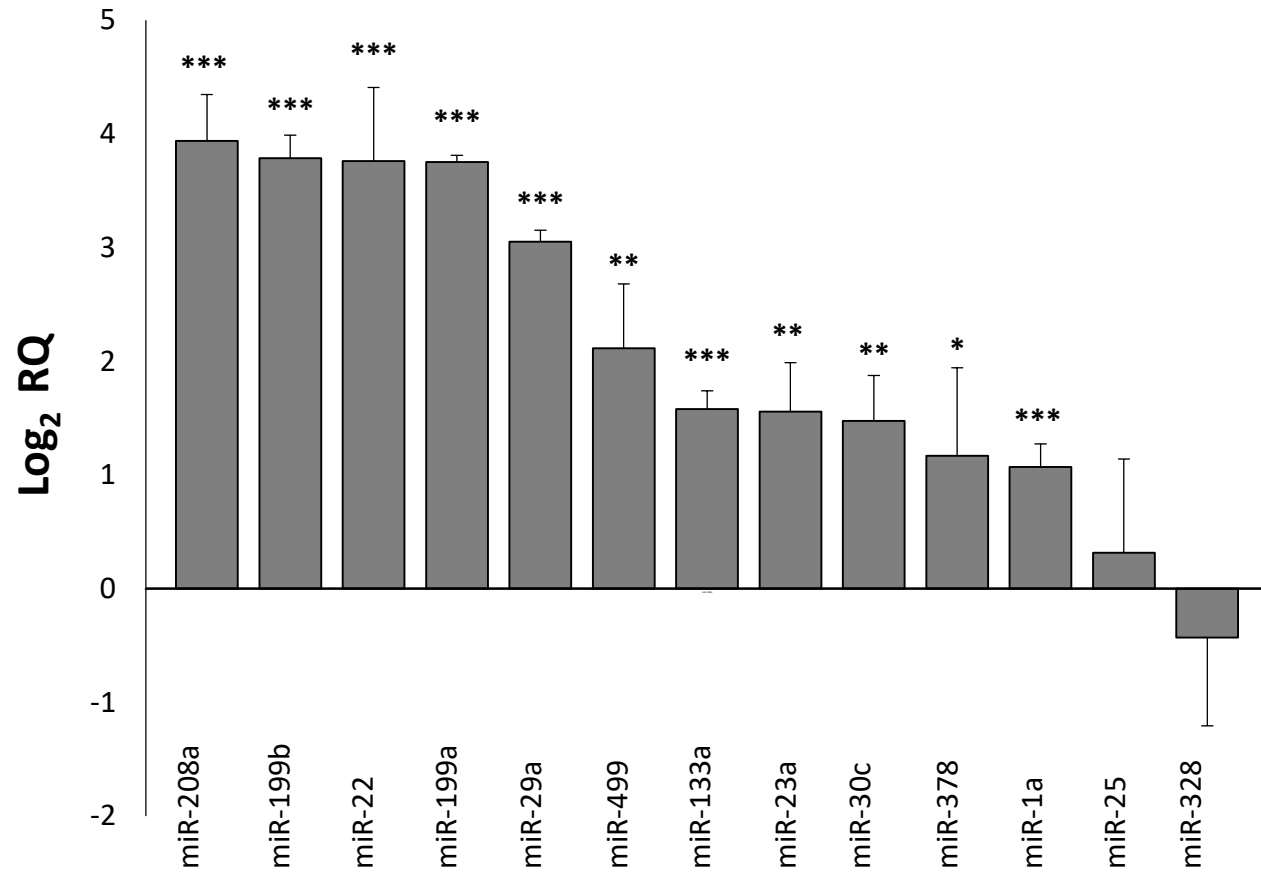
**Figure 6. Relative levels of miR-22, miR-29a, miR-133a and miR-199a in plasma samples from PA patients.** miRNA relative expression analysis was performed by qRT-PCR. All samples were from PA patients and controls older than 12 years (n=10 per group). **(A)** Representation of the mean levels of cardiomiRs and **(B)** miRNA profile for each patient. Statistical significance was determined by Student's t-test.  $**p<0.01$ .  $*p<0.05$ . RQ: relative quantity.

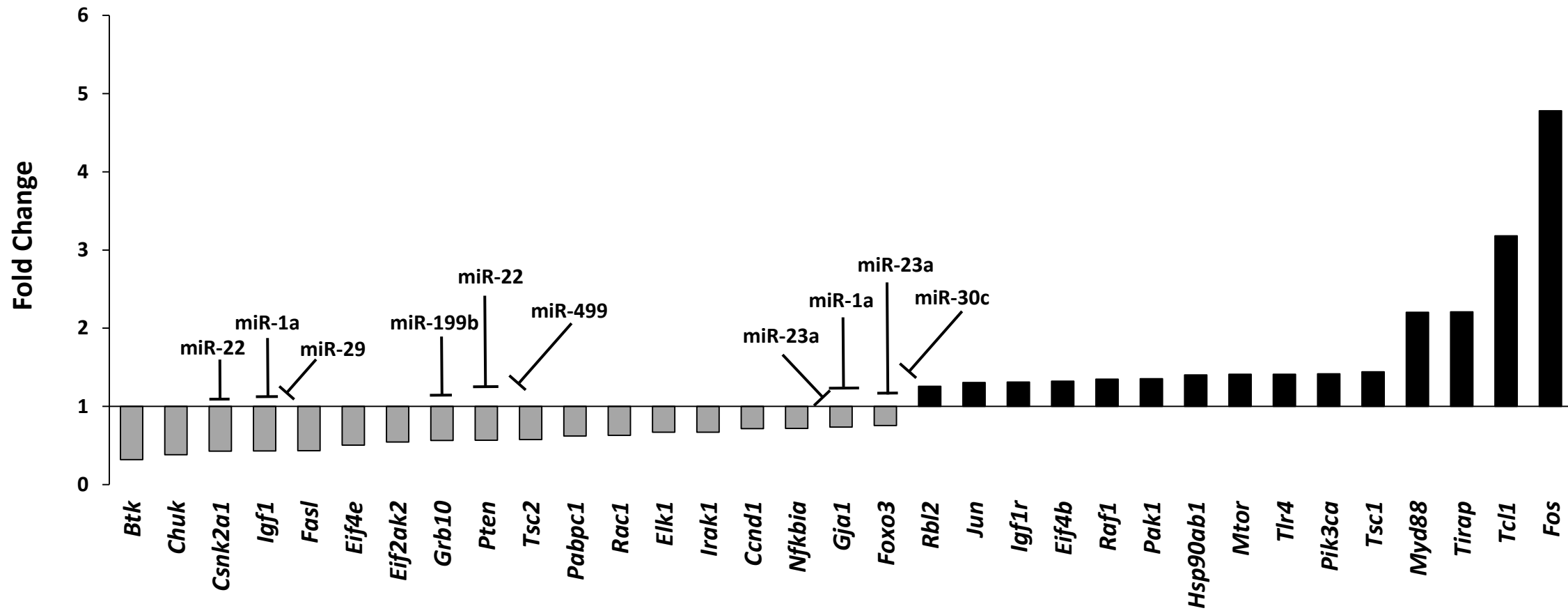
## Wild type



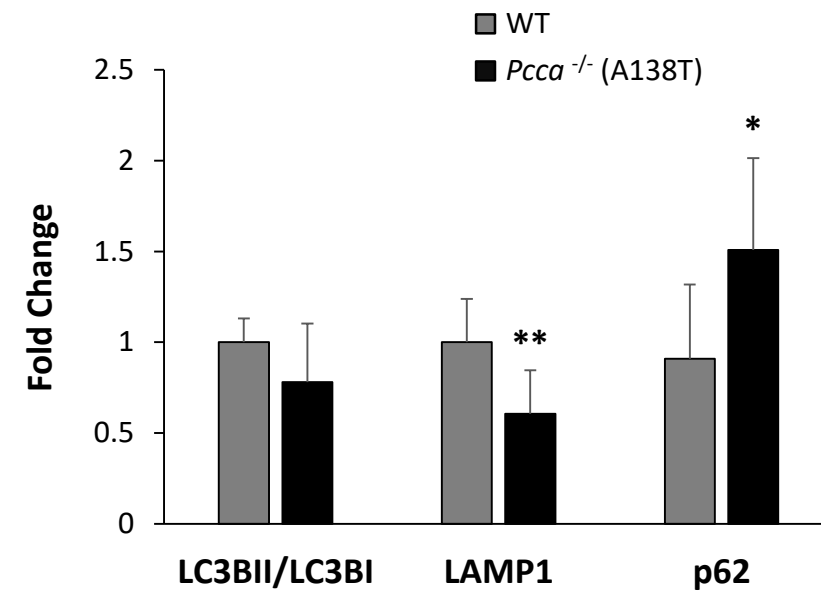
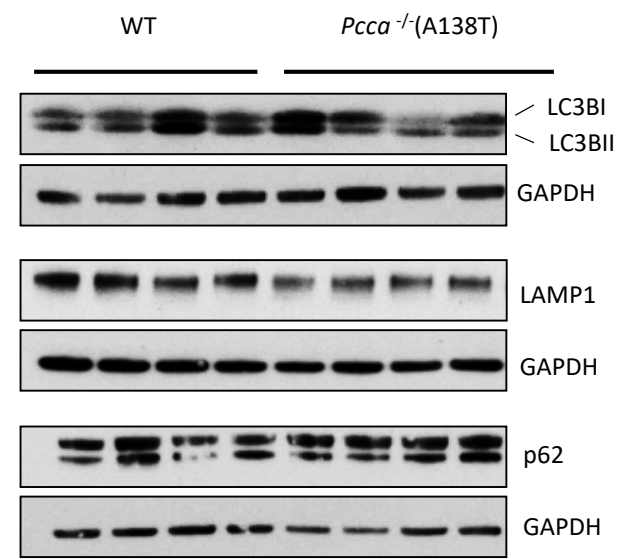
## *Pcca*<sup>-/-</sup>(A138T)



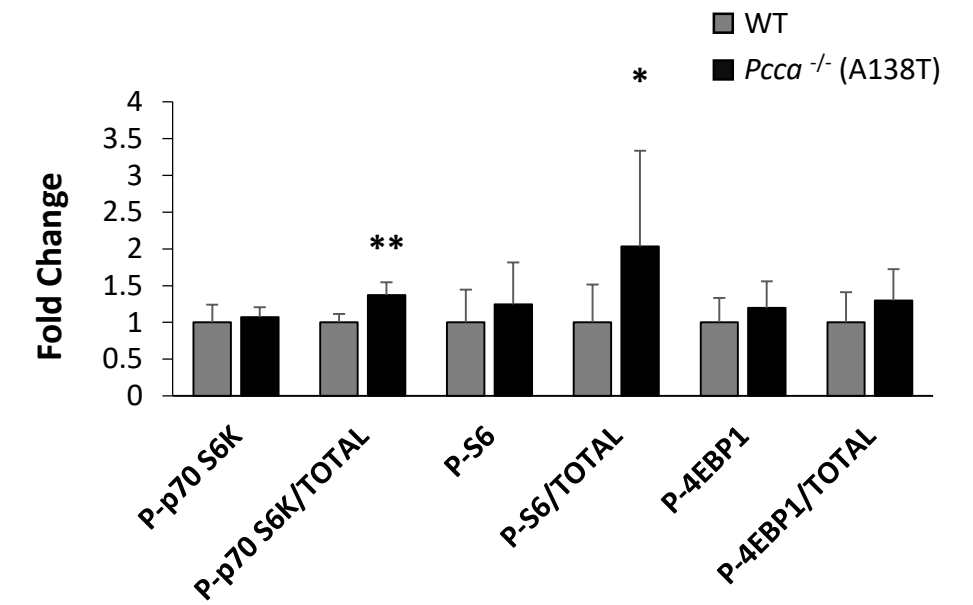
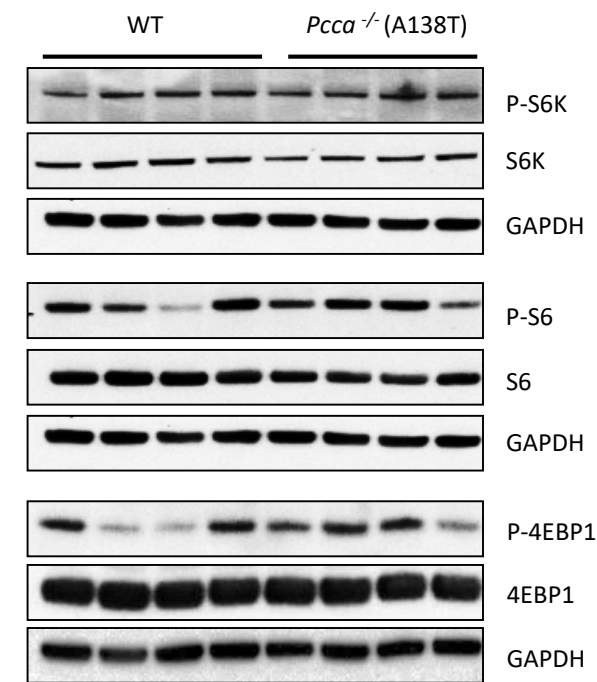




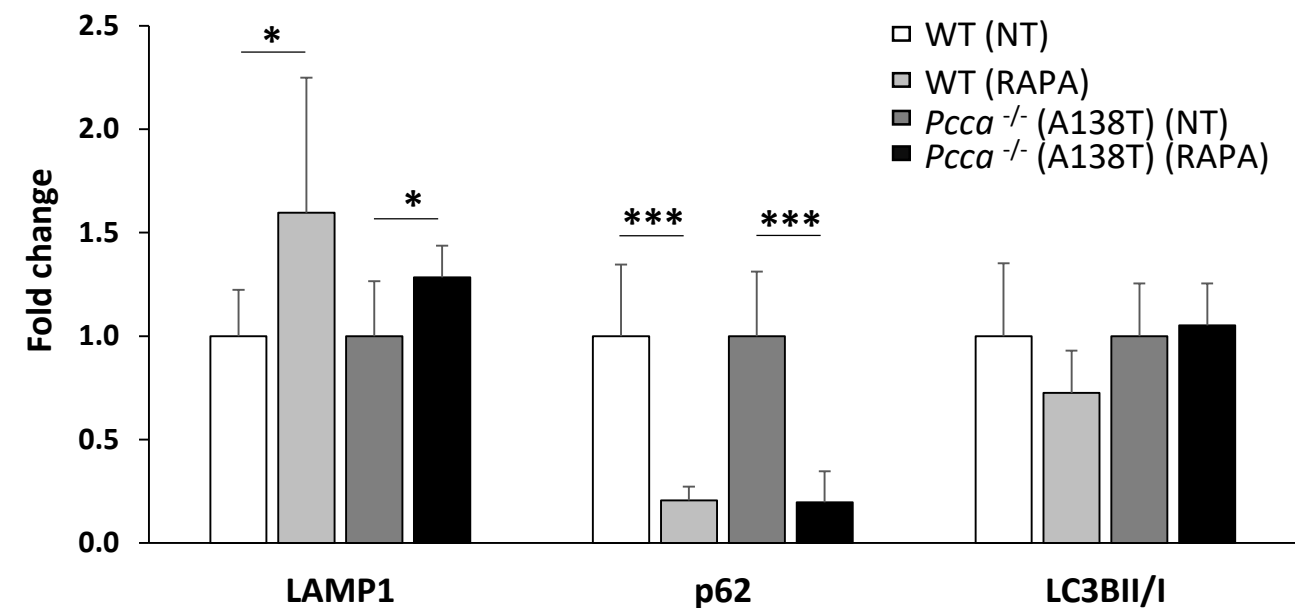
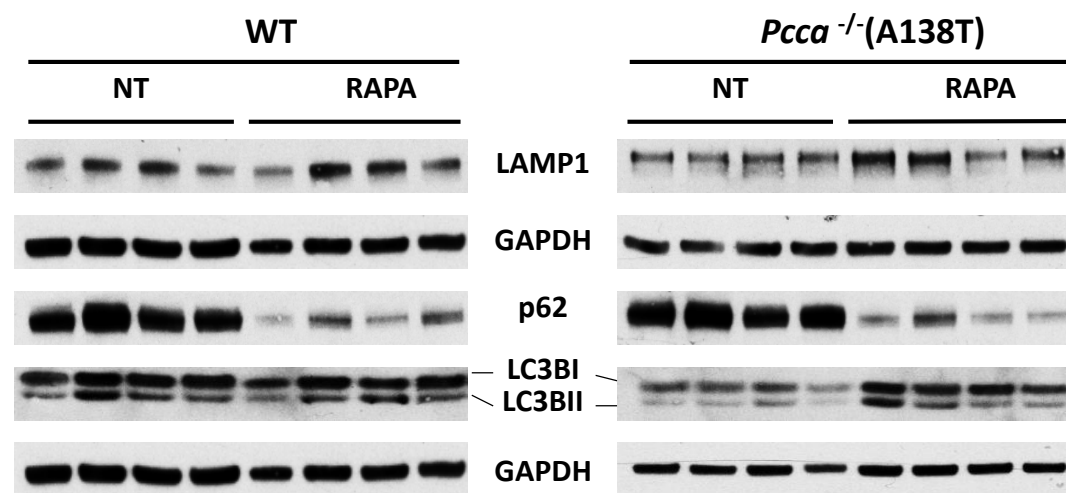
A)



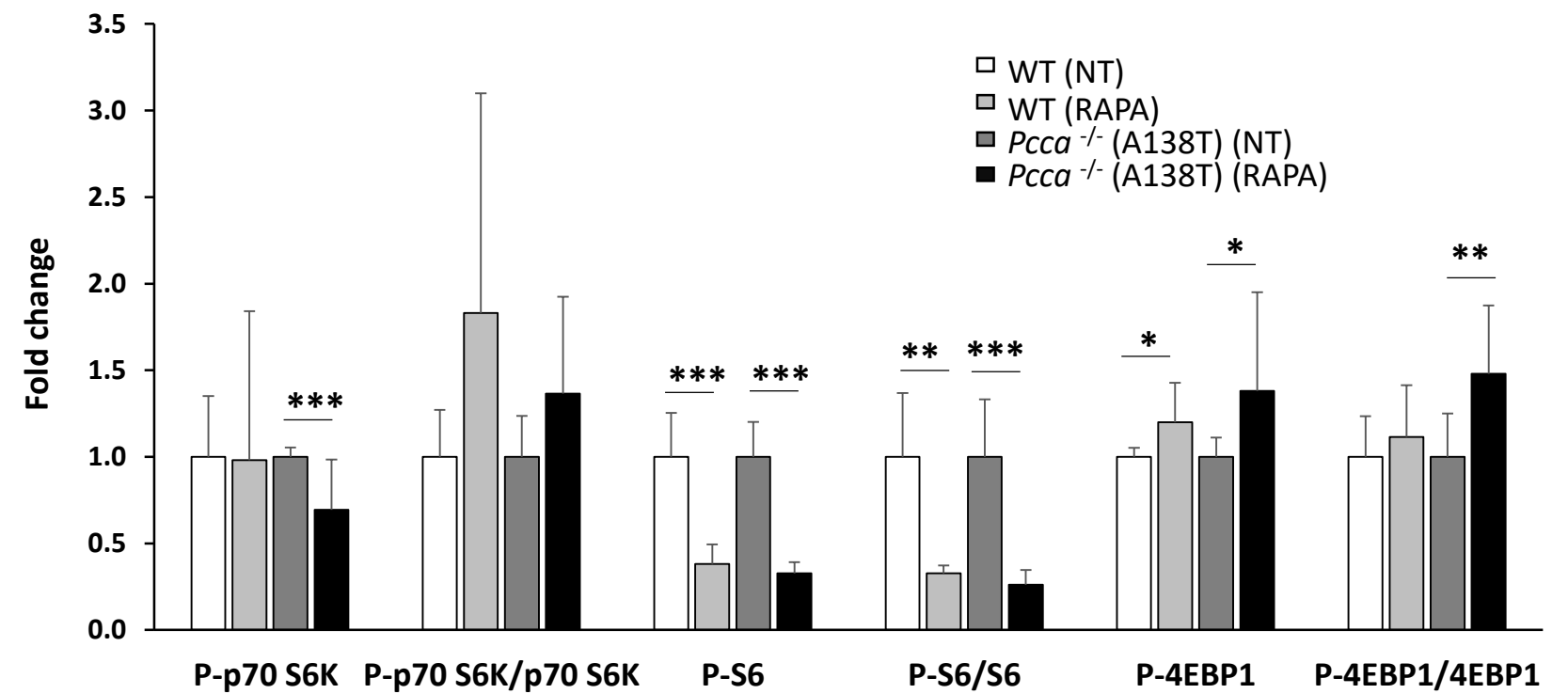
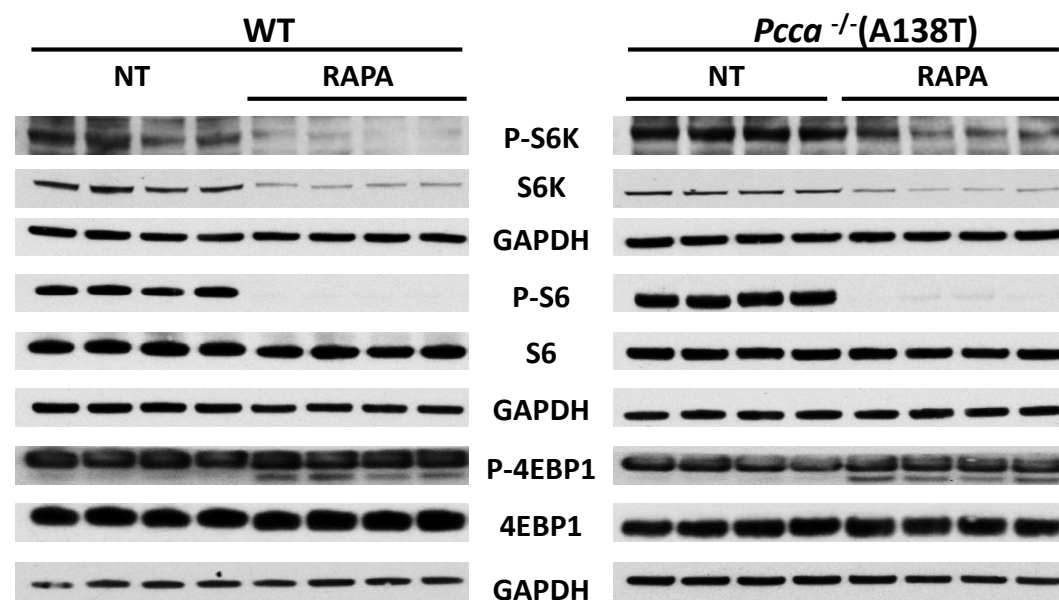
B)



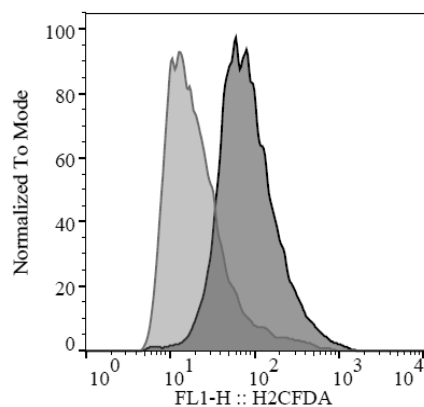
C)



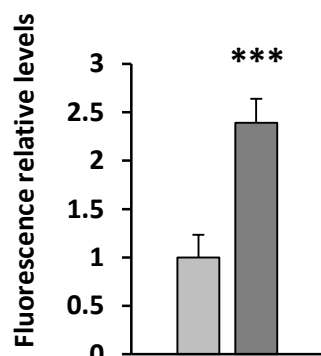
D)



A)

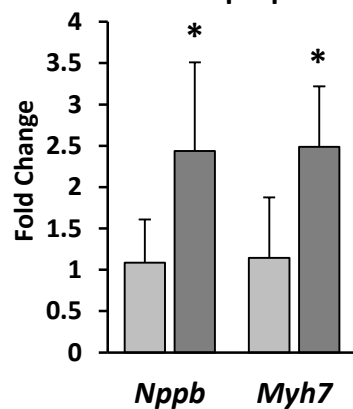


■ Non treated  
■ 5mM propionate



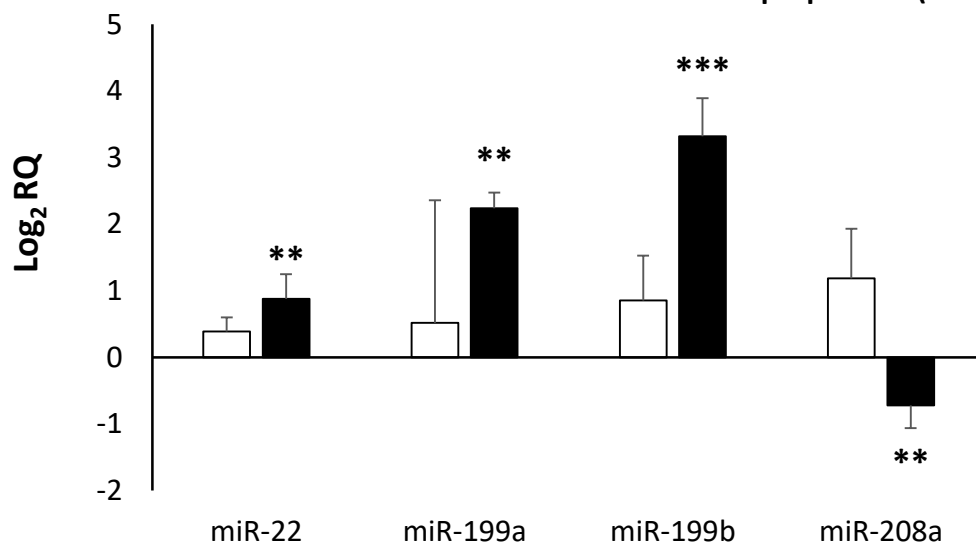
B)

■ Non treated  
■ 5mM propionate

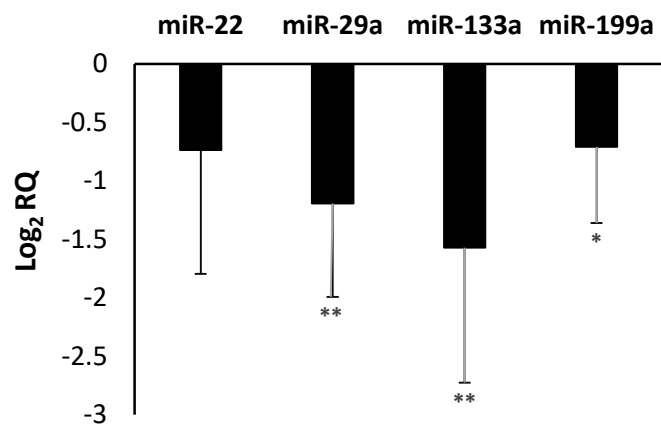


C)

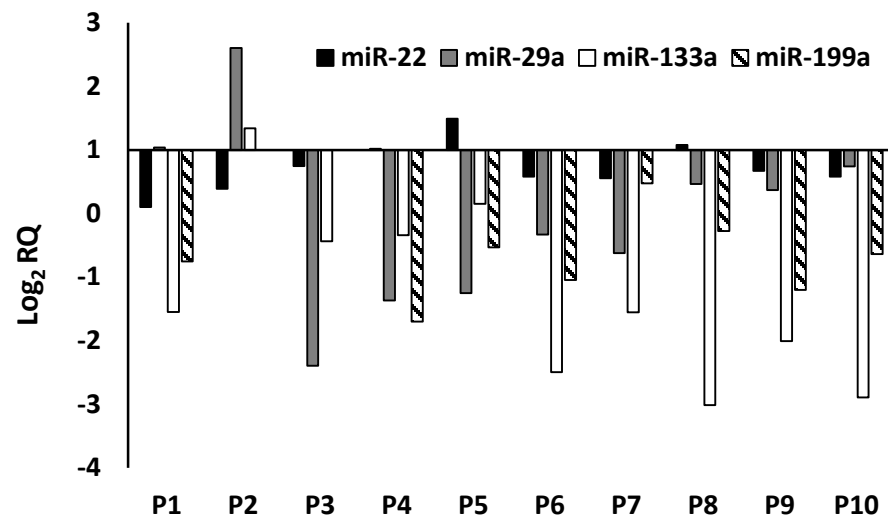
□ 5mM propionate (4 days)  
■ 5mM propionate (8 days)



A)



B)



## **SUPPLEMENTARY MATERIAL**

### **PATHOGENIC IMPLICATIONS OF DYSREGULATED miRNAs IN PROPIONIC ACIDEMIA RELATED CARDIOMYOPATHY**

Alejandro Fulgencio-Covián, Esmeralda Alonso-Barroso, Adam J Guenzel, Ana Rivera-Barahona, Magdalena Ugarte, Belén Pérez, Michael A Barry, Celia Pérez-Cerdá, Eva Richard, Lourdes R Desviat



**Supplementary Table 1. Cardiac-enriched miRNAs analyzed in PA mouse heart samples.**

<b>miRNA</b>	<b>Validated target genes</b>	<b>Role in cardiac disease</b>	<b>Signaling pathway</b>	<b>References</b>
miR-1a-3p	<i>Igf1r</i> <i>Bcl2</i> <i>Ppp2r5c</i> <i>Mef2a</i>	Hypertrophy Apoptosis Arrhythmias Fibrosis	PI3K/AKT	[1]
miR-22-3p	<i>Sirt1</i> <i>Hdac4</i> <i>Pten</i> <i>Tgfβr1</i>	Hypertrophy Apoptosis Fibrosis	PI3K/AKT	[2]
miR-23a-3p	<i>Trim63</i> <i>Foxo3a</i>	Hypertrophy	CaN/NFAT	[3]
miR-25-3p	<i>Hand2</i> <i>Serca2a</i>	Apoptosis	Ca <sup>2+</sup> homeostasis	[4]
miR-29a-3p	<i>Col3a1</i> <i>Col1a1</i> <i>Col1a2</i>	Fibrosis	-	[5]
miR-30c-5p	<i>Trp53</i> <i>Dnm1l</i>	Apoptosis	p53	[6]
miR-133a-3p	<i>Casp3</i> <i>Casp9</i> <i>Tgfb1</i> <i>Rhoa</i>	Apoptosis Fibrosis Hypertrophy	MAPK PI3K/AKT	[7]
miR-199a-3p	<i>Ppard</i> <i>Gsk3b</i>	Hypertrophy Apoptosis	PI3K/AKT mTOR	[8, 9]
miR-199b-5p	<i>Dyrk1</i>	Hypertrophy Fibrosis	CaN/NFAT	[10]
miR-208a-3p	<i>Med13</i> <i>Gdf8</i>	Hypertrophy Fibrosis	-	[11]
miR-328-3p	<i>Serca2a</i>	Hypertrophy	Ca <sup>2+</sup> homeostasis	[12]
miR-378-3p	<i>Casp3</i> <i>Igf1r</i>	Apoptosis Hypertrophy	MAPK PI3K/AKT	[13]
miR-499-3p	<i>Ppp3ca</i>	Hypertrophy Apoptosis	CaN/NFAT	[14]

## REFERENCES

- [1] Zhao Y, Ransom JF, Li A, Vedantham V, von Drehle M, Muth AN, et al. Dysregulation of cardiogenesis, cardiac conduction, and cell cycle in mice lacking miRNA-1-2. *Cell*. 2007;129:303-17.
- [2] Huang ZP, Chen J, Seok HY, Zhang Z, Kataoka M, Hu X, et al. MicroRNA-22 regulates cardiac hypertrophy and remodeling in response to stress. *Circ Res*. 2013;112:1234-43.
- [3] Lin Z, Murtaza I, Wang K, Jiao J, Gao J, Li PF. miR-23a functions downstream of NFATc3 to regulate cardiac hypertrophy. *Proc Natl Acad Sci U S A*. 2009;106:12103-8.
- [4] Wahlquist C, Jeong D, Rojas-Munoz A, Kho C, Lee A, Mitsuyama S, et al. Inhibition of miR-25 improves cardiac contractility in the failing heart. *Nature*. 2014;508:531-5.
- [5] van Rooij E, Sutherland LB, Thatcher JE, DiMaio JM, Naseem RH, Marshall WS, et al. Dysregulation of microRNAs after myocardial infarction reveals a role of miR-29 in cardiac fibrosis. *Proc Natl Acad Sci U S A*. 2008;105:13027-32.
- [6] Li J, Donath S, Li Y, Qin D, Prabhakar BS, Li P. miR-30 regulates mitochondrial fission through targeting p53 and the dynamin-related protein-1 pathway. *PLoS Genet*. 2010;6:e1000795.
- [7] Care A, Catalucci D, Felicetti F, Bonci D, Addario A, Gallo P, et al. MicroRNA-133 controls cardiac hypertrophy. *Nat Med*. 2007;13:613-8.
- [8] el Azzouzi H, Leptidis S, Dirkx E, Hoeks J, van Bree B, Brand K, et al. The hypoxia-inducible microRNA cluster miR-199a-214 targets myocardial PPARdelta and impairs mitochondrial fatty acid oxidation. *Cell Metab*. 2013;18:341-54.
- [9] Li Z, Song Y, Liu L, Hou N, An X, Zhan D, et al. miR-199a impairs autophagy and induces cardiac hypertrophy through mTOR activation. *Cell Death Differ*. 2017;24:1205-13.
- [10] da Costa Martins PA, Salic K, Gladka MM, Armand AS, Leptidis S, el Azzouzi H, et al. MicroRNA-199b targets the nuclear kinase Dyrk1a in an auto-amplification loop promoting calcineurin/NFAT signalling. *Nat Cell Biol*. 2010;12:1220-7.
- [11] van Rooij E, Sutherland LB, Qi X, Richardson JA, Hill J, Olson EN. Control of stress-dependent cardiac growth and gene expression by a microRNA. *Science*. 2007;316:575-9.

- [12] Li C, Li X, Gao X, Zhang R, Zhang Y, Liang H, et al. MicroRNA-328 as a regulator of cardiac hypertrophy. *Int J Cardiol.* 2014;173:268-76.
- [13] Fang J, Song XW, Tian J, Chen HY, Li DF, Wang JF, et al. Overexpression of microRNA-378 attenuates ischemia-induced apoptosis by inhibiting caspase-3 expression in cardiac myocytes. *Apoptosis.* 2012;17:410-23.
- [14] Wang JX, Jiao JQ, Li Q, Long B, Wang K, Liu JP, et al. miR-499 regulates mitochondrial dynamics by targeting calcineurin and dynamin-related protein-1. *Nat Med.* 2011;17:71-8.

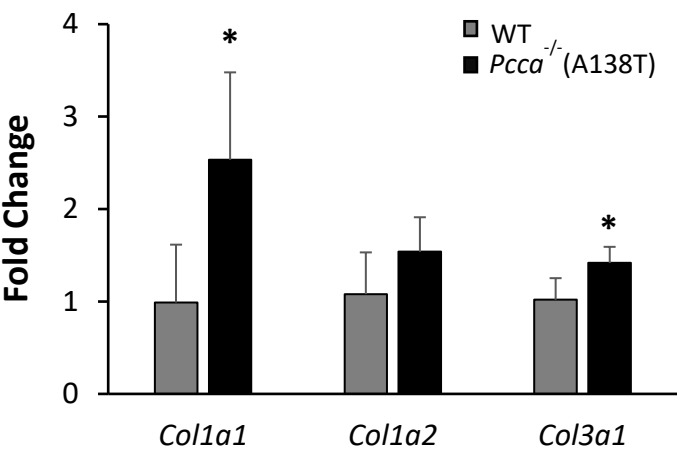
## Legends to Supplementary Figures

**Supplementary Figure 1. Relative mRNA levels of fibrotic markers *Colla1*, *Colla2* and *Col3a1*.** Gene expression analysis was performed by qRT-PCR in heart samples from wt and PA mice (5 month-old, n=5 per group). Statistical significance was determined by Student's t-test.  $*p<0.05$ .

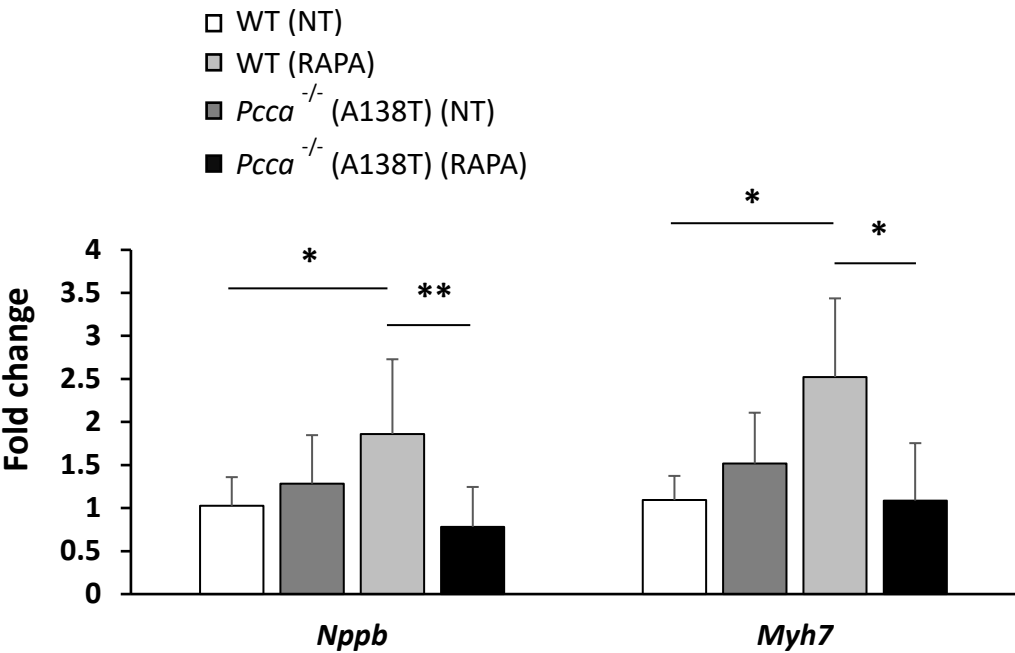
**Supplementary Figure 2. Expression of cardiac damage markers in heart of wt and PA mice after rapamycin treatment.** Expression levels of *Nppb* and *Myh7* (coding for BNP and  $\beta$ -MHC, respectively) were analyzed by qRT-PCR in 5 month-old wt and PA mice (n=9-10 per group). Statistical significance was measured by ANOVA followed by the Tukey's honestly significant difference (HSD) or Games Howell post hoc test.  $*p<0.05$ ;  $**p<0.01$ . NT: non treated; RAPA: rapamycin treated.

**Supplementary Figure 3. Expression analysis of targets of upregulated cardiomiRs.** Analysis of mRNA levels of (A) *Ppard* (miR-199a target) and (B) *Med13* (miR-208a target) was performed by qRT-PCR in wt and PA mice hearts (5 month-old, n=5 per group). (C) Analysis of protein levels of Caspase 3 and Caspase 9 was carried out by western blot using GAPDH as loading control in wt and PA mice (5 month-old, n=8 per group) and protein quantification was performed by laser densitometry. Statistical significance was determined by Student's t-test.  $*p<0.05$ ;  $**p<0.01$ ,  $***p<0.001$ .

Supplementary Figure 1



Supplementary Figure 2



Supplementary Figure 3

